



ارائه شده توسط:

سایت ترجمه فا

مرجع جدیدترین مقالات ترجمه شده

از نشریات معتبر

## Strip footing behavior on reinforced sand with void subjected to repeated loading

A. Asakereh<sup>1</sup>, S.N. Moghaddas Tafreshi<sup>2</sup>, M. Ghazavi<sup>2,\*</sup>

Received: January 2011, Accepted: August 2011

### Abstract

*This paper describes a series of laboratory model tests on strip footings supported on unreinforced and geogrid-reinforced sand with an inside void. The footing is subjected to a combination of static and cyclic loading. The influence of various parameters including the embedment depth of the void, the number of reinforcement layers, and the amplitude of cyclic load were studied. The results show that the footing settlement due to repeated loading increased when the void existed in the failure zone of the footing and decreased with increasing the void vertical distance from the footing bottom and with increasing the reinforcement layers beneath the footing. For a specified amplitude of repeated load, the footing settlement is comparable for reinforced sand, thicker soil layer over the void and much improved the settlement of unreinforced sand without void. In general, the results indicate that, the reinforced soil-footing system with sufficient geogride-reinforcement and void embedment depth behaves much stiffer and thus carries greater loading with lower settlement compared with unreinforced soil in the absent of void and can eliminate the adverse effect of the void on the footing behavior. The final footing settlement under repeated cyclic loading becomes about 4 times with respect to the footing settlement under static loading at the same magnitude of load applied.*

*Keywords: Repeated loads; Void; Geogrid reinforcement; Laboratory test; Strip footing; Footing settlement*

### 1. Introduction

Underground voids located in the failure zone of the footing can cause serious engineering problem leading to instability of the foundation and severe damage to the superstructure. If the void is located below the footing at shallower depth, the consequence can be very costly and dangerous. They may occur as a result of settlement of poorly compacted trench backfill; natural caves, tunnels, pipes, water and gas networks and old conduits. Because of the population growth and increasing demand for extending the urban outspread to the areas that might have previously undergone mining operations, the mining cavities (voids and old conduits) are becoming a growing concern for geotechnical engineers dealing with foundation stability issues, especially above soft ground beds.

Many researchers have studied the performance of footing on unreinforced soil with void under static loads [1- 4]. Badie

and Wang [2] performed a theoretical and experimental analysis on a model footing above clayey soil to investigate the stability of spread footings situated above a continuous void. The results of this study implied that there is a critical region under the footing and only when the void is located within that critical region, the bearing capacity of the footing varies considerably with the void location. When the stability and load-carrying characteristics of footing are affected by void, various alternatives such as filling the void with competent material; using piles to transmit the load to an acceptable soil or rocks at the bottom of the void; and relocation of the foundation so that it is placed away from the void may be considered. Among these, the footing relocation is relatively easy and costly justified. However, it is only practical if sufficient space is available. Other alternatives may be considerably expensive or impossible and infeasible for the existing conditions.

In recent decades, due to ease of construction and ability to improve load-carrying characteristics under static loads, geosynthetics reinforced soil has been widely of interest to geotechnical engineers in various applications [5-21].

Theoretical and experimental studies have been carried out on dynamic characteristics of shallow foundations supported on unreinforced soil to discover the role of load

\* Corresponding Author: ghazavi\_ma@kntu.ac.ir

<sup>1</sup> Department of Civil Engineering, K.N. Toosi University of Technology, Valiasr St., Mirdamad Cr., Tehran, Iran

<sup>2</sup> Associate Professor Department of Civil Engineering, K.N. Toosi University of Technology, Valiasr St., Mirdamad Cr., Tehran, Iran

cycles on footing settlement [22-24]. For footings on reinforced soil under repeated loads, only a few relevant studies have been reported [25, 26, 27, 28, 29]. Das and Maji [30] and Das [31] conducted laboratory model tests and observed that under repeated low frequency loading, footings on geosynthetics reinforced medium dense soil experience less settlements than static loading. Moghaddas Tafreshi & Dawson [21] carried out a series of laboratory model tests on strip footings supported on 3D and planar reinforced sand beds with the same characteristics of geotextile under a combination of static and repeated loads. They indicated that substantial improvement in the footing system performance can be achieved with the provision of reinforcement and also for the same quantity of geotextile material; the 3D reinforcement system behaves much stiffer and causes less settlement than does the equivalent planar reinforcement system.

In the case of footing supported by reinforced soil bed with a void under monotonic loads, several researches were carried out [32, 33, 34, 35]. Das and Khing [32] used a laboratory model test to determine the improvement of the bearing capacity supported by a stronger sand layer underlain by a weaker clay layer with a continuous rectangular void located below the centerline of the foundation. They reported that the bearing capacity is generally reduced due to the existence of a void and it substantially increases with only one layer of geogrid. Sireesh et al. [35] carried out a series of laboratory scale model tests on a circular footing supported by geocell reinforced sand beds overlying a clay bed with a continuous circular void. They reported that substantial improvement in the performance can be obtained with the provision of a geocell mattress, of adequate size, over the clay subgrade with void.

Since footings subjected to cyclic loads are occasionally situated above the void, understanding the effect of the void on the footing performance and also the beneficial effect of the soil reinforcement in negating the decreasing effect of the void on the footing settlement is of great importance. Also, the above literature indicates that there is still a major lack of comprehensive studies on the behavior of footings on reinforced soil with void under repeated loading. In order to contribute to develop a better understanding of such studies, in this research, a series of laboratory and pilot-scale tests under monotonic and repeated loads were performed to evaluate the settlement of a strip footing above a void supported on reinforced relatively dense sand with planar geogrid reinforcement. The testing program was planned to investigate the response of footings constructed on reinforced sand and unreinforced sand with void and subjected to repeated loading. In particular, it is aimed to demonstrate the benefits of geogrid reinforcement application over soil unreinforced conditions. The effect of the number of the reinforcement layers ( $N$ ) below the footing base, the embedment depth of the void ( $H/D$ ) on decreasing the negative effect of the void on footing settlement and also the ratio of repeated load intensity to applied static load, and the number of load cycles rapidity with which steady-state conditions arise are investigated.

## 2. Testing apparatus

The testing apparatus used in the current study is shown in Fig. 1. This apparatus seems to be able to accommodate the model strip footing on void with a soil of predetermined uniform density. It generally consists of four main parts namely loading system, testing tank, soil preparation device, and data acquisition system. A brief description of each part will be given subsequently.

### 2.1. Loading system

The loading system consists of a frame, a hydraulic cylinder, and a controlling unit. The loading frame comprises two stiff and heavy steel columns with 1600 mm height and a horizontal beam with 1270 mm length, which supports the hydraulic cylinder with internal diameters of 80 mm. The hydraulic cylinder may produce monotonic or cyclic loads depending on the intensity of the input compressed oil. The cyclic vertical loads with different amplitudes (up to 10 kg/cm<sup>2</sup>), frequencies (up to 1 Hz), and number of load cycles can be produced and controlled by the unit control.

### 2.2. Testing tank

A strip footing over a continuous concentric void in a soil-bed system is included in the class of structures that can be treated in a state of plane strain since they have a longitudinal length  $z$ , much bigger than the other two dimensions in the  $x$  and  $y$  directions. In small-scale test, the plane strain condition could be achieved either by building the model with the smooth  $x$ - $y$  faces in order to prevent any friction that could cause distortion in the longitudinal direction or by taking the  $z$  dimension such that the end effects do not interfere with the behavior of the middle test section.

The testing tank is designed as a rigid steel box, 1000 mm in

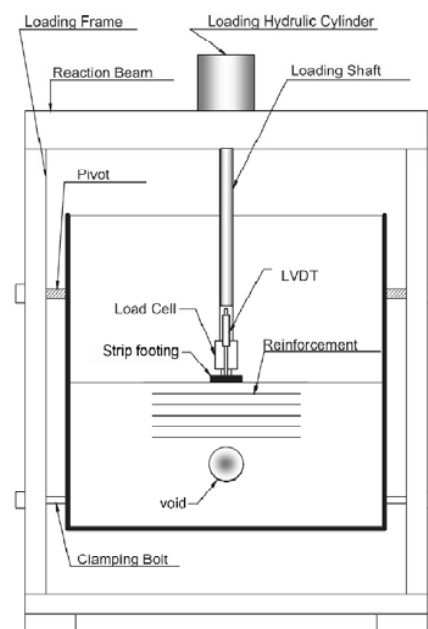


Fig. 1. Schematic view of testing apparatus

length, 1000 mm in height, and 220 mm in width (in the  $z$  direction), encompassing the reinforced soil and model void (Fig. 2), which stands vertically along its square face while testing is in progress (Figs. 1-3). The testing tank has a smooth back and front faces and is sufficiently rigid to impose a plane strain state on the soil. The back face of the tank consists of a steel plate of 10mm thickness, which is permanently fixed to the channel plates and its front face consists a plexy glass of 20 mm thickness, which can be removed during test preparation. The front face is supported by a strong solid beam of the box section of 30×60 mm to prevent undesirable movement of the front side to maintain plane strain condition (Fig. 3).

The testing tank is connected to the sides' columns loading frame by means of two horizontal pivots which can be rotated and be fixed in the horizontal or vertical directions, when required. The testing tank must have the ability of being set horizontally during the preparation stages and of being set vertically during the loading stage as described in section 4. After completing the preparation and before applying the load, the tank is set in the vertical position by rotating it 90 degrees quite gently. To allow the visual observations of the sand-void system, as well as the photo scanning, the front face of the tank has been made of a plexy glass, which can be removed during the preparation stage.

### 2.3. Soil preparation device

In order to provide experimental control and repeatability of the tests, the raining technique was used to deposit the soil in

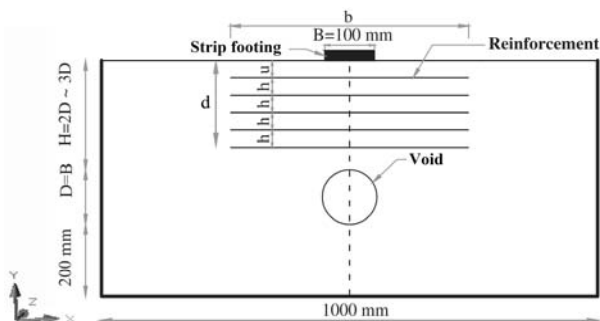


Fig. 2. View layout of trench (not in scale)

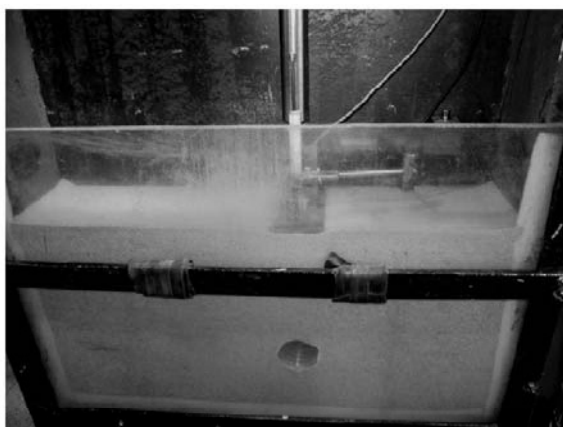


Fig. 3. General view of the testing tank together with its attachments

the testing tank at a known and uniform density [36]. A moveable steel tank and a moveable perforated steel plate was provided for raining the sand inside the testing tank. It may be mounted above the testing tank to pour the sand from a specified height. The height of raining to achieve the desired density was determined a priori by performing a series of trials with different heights of raining. Sand was then rained from a pre-calibrated height to consistently maintain a relative density of 73% in all the tests.

### 2.4. Data acquisition system

This system was developed in such a way that all loads, displacements, and times could be read and recorded automatically. An S shaped load cell with an accuracy of  $\pm 0.01\%$  full scale is also used and placed between the loading shaft and soil surface with a capacity of 50 kN to precisely measure the pattern of the applied load on the trench surface. Two linear variable differential transducers (LVDTs) with an accuracy of 0.01% of full range (100 mm) are placed on the two sides of the footing model to provide an average settlement of the soil surface,  $s$ , during the repeated loads. To ensure an accurate reading, all of devices are calibrated prior to each test. The general view of the testing tank and all relevant attachments at the beginning of a test are shown in Fig. 3.

## 3. Materials

### 3.1. Sand

Relatively uniform silica sand with grain size ranging 0.07 to 1.24 mm was used. The grain size distribution of the sand is shown in Fig. 4. The sand classified as SP in the Unified Soil Classification System has properties presented in Table 1.

### 3.2. Geogrid

The geogrid used in this research was made by an Iranian company with engineering properties given by the manufacturer as presented in Table 2.

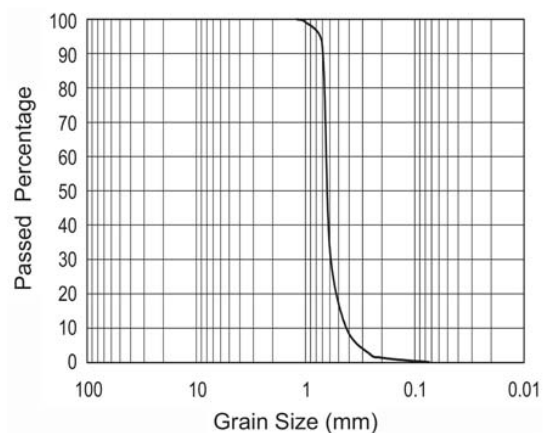


Fig. 4. Particle size distribution

**Table 1.** Physical properties of soil

| Description                         | Value |
|-------------------------------------|-------|
| Coefficient of uniformity, $C_u$    | 1.51  |
| Coefficient of curvature, $C_c$     | 1.29  |
| Effective grain size, $D_{10}$ (mm) | 0.4   |
| $D_{30}$ (mm)                       | 0.6   |
| Medium grain size, $D_{50}$ (mm)    | 0.64  |
| $D_{60}$ (mm)                       | 0.65  |
| Maximum void ratio, $e_{max}$       | 1.12  |
| Minimum void ratio, $e_{min}$       | 0.55  |
| Moisture content (%)                | 0     |
| Specific gravity, $G_s$             | 2.67  |
| Friction angle, (degree)            | 38.6  |

**Table 2.** Engineering properties of HDPE geogrid

| Description                            | Value |
|--|-------|
| Thickness (mm)                         | 5.2   |
| Mass per unit area ( $\text{kg/m}^2$ ) | 0.695 |
| Ultimate tensile strength (kN/m)       | 5.8   |
| Aperture size (mm)                     | 27×27 |

#### 4. Preparation of model test

The raining technique was used to deposit the soil into the tank. This method allows the void circular cross-section to be maintained without having to introduce the moulds that compaction methods usually require. To provide the stability of the void in a circular shape, a 100 mm diameter flexible can with 0.6 mm thickness and 218 mm length (On each side of the tank, in  $z$  direction, a 1 mm wide gap was provided to prevent contact between the footing and the front and back faces of the tank). The model void (flexible can) has an insignificant bending stiffness in air but supports the sand due to the lateral confinement when embedded in the trench. On the other hand, when the can uses as a void in the soil trench, it acts as a flexible lining and produces resistance against the soil pressure. It is due to soil confining pressure at the shoulders and sides of the void (flexible can) and the void would not be easily closed due to static and repeated loads applied on the footing surface. This was checked carefully by observation during tests and thus might be regarded as a relatively real void. The bending stiffness of the plastic can,  $EI$ , is measured by performing a bending test. The measured value of  $EI$  was found to be about  $160 \text{ kg.cm}^2$  which is quite insignificant. This again justifies that the void can be considered a relatively real void. The void diameter ( $D$ ) and the footing width ( $B$ ) were both equal to 100 mm in all tests.

In order to prepare the model test, the testing tank should be rotated to the horizontal position to deposit the soil in the tank by raining, perpendicularly to the longitudinal axis of the pipe [37]. Before using the hopper for depositing the soil in the tank, the raining device was calibrated using different heights of pouring and different perforated plates. Consequently, the required height of pouring and perforated plate to get the desired

density can be selected for a special test. The embedment depth of the flexible lining was adjusted by limiting the top of the tank by means of a temporary wooden wall. The free end of the lining was sealed, the geogrid layers were placed at the required positions above the void (or below the soil surface), and the soil was poured to the tank using the raining technique. Finally, the surface of the soil was leveled carefully and the plexy glass was placed and fixed and the testing tank was rotated quite gently to the vertical position. To ensure that the calibrated raining produced was correct and the proper relative density and that the density was maintained while the tank was rotated, the soil density was measured after rotating the tank in several tests. It was found that the maximum difference in the soil density after raining and rotation was about 1%-2%. This small difference could be acceptable from geotechnical viewpoint. At this stage, the model foundation, as soil surface loading (a steel rigid plate of 218 mm length, 100 mm width, and 20 mm thickness), was centered in the tank, with a length of the footing parallel to the width of the tank, in the  $z$  direction. The base of the model footing was made roughened by covering it with epoxy glue and rolling it in sand. In order to provide vertical loading alignment, a small hemi-spherical indentation was made at the centre of the footing model. A load cell was placed on the loading shaft to record the applied loads and its lower end equipped with a hemispherical protrusion that engaged with the seating on the footing. A LVDT was placed on the footing model accurately to measure the settlement of the footing during the loading. The static load was applied at a rate of 1.0 kPa per second until the failure is reached. In the absence of a clear-cut failure, the footing was loaded to reach a constant applied stress value.

#### 5. Pattern of applied repeated load

Foundations are periodically subjected to a combination of static and repeated loads in many circumstances such as earthquakes, wind forces in tall buildings, pile construction, machine vibrations and etc, hence, the investigation and design of footings under dynamic loadings still remains a challenging task for geotechnical engineers. These foundations require special attention due to the presence of both static loads due to weight (or external load) and also dynamic loads due to vibrating components. While dynamic loads are generally small, they are applied repetitively over a very large number of cycles, resulting in footing settlement, sometimes, leading to the soil failure.

Fig. 5 shows a typical time history of applied load on the footing. As seen, the footing is subjected to a pre-specified static load of intensity,  $q_s$ , applied at a rate of 1.0 kPa/s, after which a repeated load having amplitude of  $q_d$  is superimposed to the static load. Before applying the repeated load, the static load is kept constant until no further settlement occurs or the rate of settlement becomes negligible. During the tests the static load would be permanently applied on the footing while the repeated load was brought to zero at the end of each cycle. Sinusoidal load cycles with a frequency of 1 Hz would be continued until the rate of change of total settlement drops to an insignificant amount or, alternatively, excessive settlement and unstable behavior is observed.

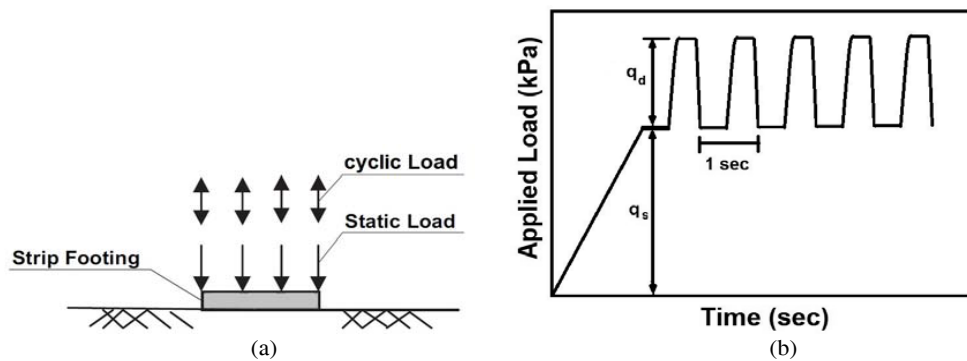


Fig. 5. Typical time history of initial static and repeated loading on footing.

## 6. Test parameters and testing program

The geometry of the test configurations considered in these investigations is shown in Fig. 2. Also the details of static and repeated tests are given in Table 3. Some 76 tests in different series were planned and carried out in this research to study the effect of embedment depth of the void ( $H/D$ ), the number of reinforcement layers ( $N$ ), the ratio of repeated load intensity to the ultimate load ( $q_d/q_u$ ), and the number of load cycles on the behavior of footing on reinforced sand with void. Test series were carried out on unreinforced and reinforced sand with or without void to quantify the improvements due to reinforcements. Among these 76 tests, 12 tests were repeated carefully to examine the performance of the apparatus and the accuracy of the measurements. The results obtained depicted a close match between results of the two or three trial tests with maximum differences of around 10%. This difference is considered to be small and is subsequently neglected. It demonstrates that the procedure and technique adopted can produce repeatable tests within the bounds that may be expected from geotechnical testing apparatus.

All variables used to describe the tests are expressed in non-dimensional form with respect to the footing width. These are  $u/B$ ,  $b/B$ ,  $H/D$ , and  $q_d/q_u$ , where  $u$  is the distance between the footing bottom and the first geogrid layer,  $h$  is the distance between two subsequent geogrid layers,  $B$  is the foundation width,  $H$  is the embedded depth of the void, and  $D$  represents the void diameter. A value of 0.35 was chosen for  $u/B=h/B$  as found by Moghaddas Tafreshi and Khalaj [28] to be the best. They performed tests on buried pipes under traffic loads and found 0.35 as the best value. The length of geogrid,  $b$ , was held kept constant at  $b/B=6$  in all tests. It is noted that the above value for  $u/B$  and  $h/B$  was also found by Yoon et al. [7], Ghosh et al. [9], and Moghaddas Tafreshi and Dawson [21] to be the best to obtain the maximum foundation

bearing capacity and minimum settlement.

The static and repeated tests were conducted in four series of tests to investigate the following cases (Table 3):

- the bearing capacity of strip footing on reinforced and unreinforced sand with void at different depths depicted by  $H/D$  (static tests)
- the effect of the embedment depth of the void ( $H/D$ ) to vanish the void effect on footing system under repeated loads
- the effect of the number of reinforcement layers ( $N$ ) to vanish the void effect under repeated loads
- the effect of load cycles and the ratio of repeated load intensity to the ultimate load ( $q_d/q_u$ ), and
- to compare the footing settlement under static and repeated loads at the same load intensity

A static load test was carried out on footing on unreinforced sand and without void to provide a reference load capacity to investigate the effects of footing improvement due to soil reinforcement. In a static test, the ultimate static load capacity of unreinforced sand was found to be  $q_u=300$  kPa (Fig. 6). A factor of safety,  $FS=q_u/q_s=3$  was adopted to define  $q_s$  as 100 kPa, being the static pre-loading applied prior to cyclic loading in subsequent test series. This value of factor of safety was selected as being the minimum value likely to be used in practical applications. The values of additional dynamic load,  $q_d$  (Fig. 5) were selected as 10, 20, and 30% of  $q_u$  (i.e.,  $q_d/q_u=10\%$ , 20% and 30%). These values are deemed appropriate - the lower two encompassing stresses likely to be experienced in many earthquakes or due to the loading of vibrating machines resting on foundations, while the value of 30% represents an extreme occurrence. The value of  $q_d/q_u=30\%$  provides the safety factor of 1.58 ( $FS=q_u/(q_s+q_d)=300/(100+90)=1.58$ ). This value of factor of safety,  $FS$  satisfies the recommended value of  $FS$  by Code of Practice. The safety factor,  $FS$  for the dynamic loading, according to the relevant Code of Practice should be selected at least 1.5.

Table 3. Scheme of the static and repeated tests for unreinforced and reinforced sand

| Test series | Type of tests | Type of reinforcement       | $q_d/q_u$ (%) | $H/D$         | $N$           | $u/B$ | $b/B$ | No. of tests |
|-------------|---------------|-----------------------------|---------------|---------------|---------------|-------|-------|--------------|
| 1           | Static        | Unreinforced                | --            | No void       | --            | --    | --    | *1           |
| 2           | Static        | Reinforced and unreinforced | --            | 2.0, 2.5, 3.0 | 0, 1, 2, 3, 4 | 0.35  | 6.0   | *15          |
| 3           | Repeated      | Unreinforced                | 10, 20, 30    | No void       | 0             | --    | --    | *3           |
| 4           | Repeated      | Reinforced and unreinforced | 10, 20, 30    | 2.0, 2.5, 3.0 | 0, 1, 2, 3, 4 | 0.35  | 6.0   | *45          |

(\*Indicates duplicate tests performed to verify the repeatability of the test data)

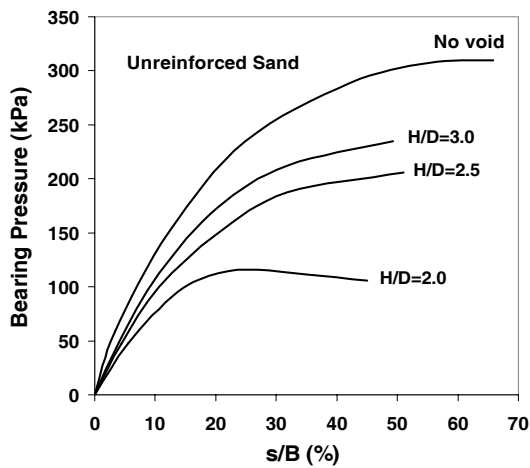


Fig. 6. Variation of bearing pressure with settlement for footing on unreinforced sand with and without void at different void embedment depth

## 7. Results and discussions

In this section, the tests results of the laboratory model are presented with a discussion highlighting the effects of the different parameters. The value of bearing pressure of the footing on unreinforced sand and on geogrid-reinforced sand under monotonic load and also the settlement of the footing under the combinations of static and repeated load (Fig. 5) has been obtained as described in Table 3. The presentation of all results would make the paper lengthy. Therefore, only a selection is presented.

### 7.1. Static tests Results

Fig. 6 presents the bearing pressure-settlement behavior of both unreinforced foundation without and with a void at different locations from the footing bottom. In the case of the void placed at  $2D$  ( $H/D=2.0$ ), it is apparent that the bearing capacity failure has taken place at a settlement of about 20% of footing width ( $s/B=20\%$ ), while in other depths of  $H/D=2.5$  and  $3.0$  and without void, no clear failure point is observed. However, an increase in embedded depth of the void leads to an increase in the footing bearing pressure but not equal with no void case. This is obvious because when the void is located well far from the footing bottom, the soil thickness underneath the footing can accommodate more shear strain before failure. Also, when embedded depth of the void increases, the failure is observed at settlements greater than 20% with ambiguous post-failure in the bearing capacity. Since no clear bearing capacity failure is observed, it is probable that no yield condition is found at conventional stress levels. At this range of settlement, for footing on the sand, heave of the fill surface starts (the results not reported here).

Fig. 7 presents the bearing pressure-settlement behavior of footing on both unreinforced and reinforced sand at different embedded depths of void. It may be clearly observed that, with increasing the number of reinforcement layers, both stiffness and bearing pressure (bearing pressure at a specified settlement) considerably increase, irrespective of

the void embedded depth. In unreinforced sand and for the void located at  $H/D=2.0$  with one layer of reinforcement ( $N=1$ ), it is apparent that the bearing capacity failure has taken place at a settlement around to 20-25% of the footing width; while no clear failure point is evident for the more reinforcement ( $N \geq 2$ ). In cases where  $H/D=2.5$  and  $3.0$ , for both unreinforced and reinforced sand, no clear failure point is evident. This is because with increasing  $H/D$ , the footing

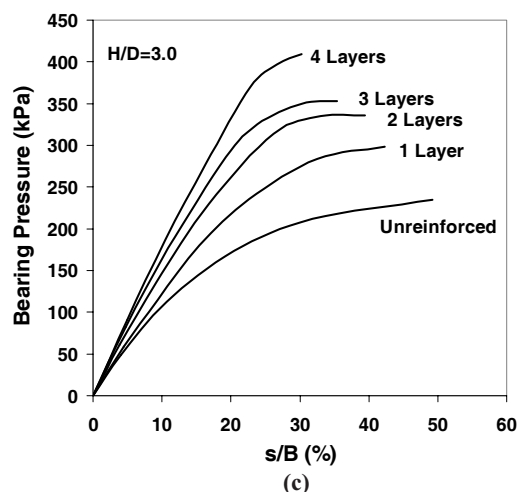
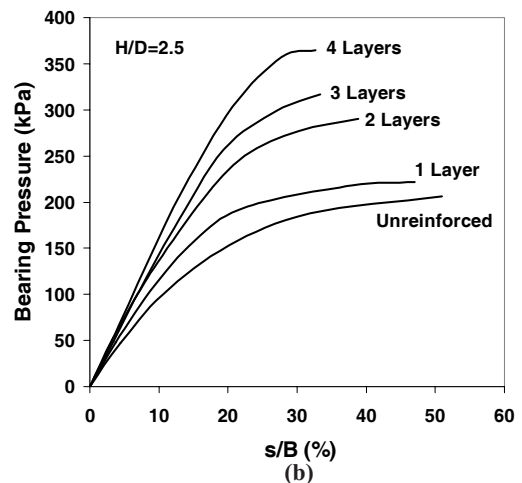
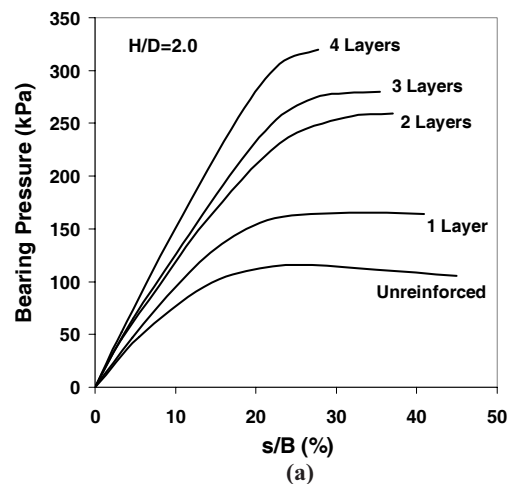


Fig. 7. Variation of bearing pressure with settlement for foundation on both unreinforced and reinforced soil for different void embedment depths, (a)  $H/D=2.0$ , (b)  $H/D=2.5$ , and (c)  $H/D=3.0$

bearing pressure-settlement pattern moves towards that of footing resting on unreinforced soil with no void. Beyond a settlement of 20%, there is a considerable reduction in the slope of the pressure-settlement curve. However, for sand reinforced with  $N=1$  and for embedded depth of  $H/D=2.0$  and 2.5, the failure is observed at settlements of 20% with clear post-failure reductions in the bearing capacity. At this range of settlement, heave of the fill surface starts. It is attributable to the soil reinforcement composite material breaking locally in the region under and around the footing, because of high deformation induced by the large settlement under the footing. This leads to a reduction in the load carrying capacity of the footing indicated by softening in the slope of the pressure-settlement response (Fig. 7). The foundation bed continues to take additional load through mobilization of its rigidity and anchorage derived from the adjacent stable soil mass, thereby giving rise to the improved performance. Because no clear bearing capacity failure has been observed, even at a settlement ratio of  $s/B=25\%$ , it is probable that no yield condition is found at conventional stress levels.

## 7.2. Cyclic tests Results

### 7.2.1. General behavior of the footing settlement under cyclic loading

Fig. 8 presents the variation of peak footing settlement with number of load cycles under cyclic loading for three values of cyclic stress ratio,  $q_d/q_u$ , unreinforced sand, and no void condition. As observed, with increasing the value of  $q_d/q_u$ , the footing settlement increases. The large portion of the footing settlement was observed in the first 500 cycles compared to the total settlement recorded after all cycles due to gradual soil compaction. Afterwards, the settlement rate decreases and finally approaches a relatively constant value. Generally due to excessive settlement, the soil has damping behavior by increasing the load cycles and the slope of settlement curve tends to reduce. In this case, it can be said that the stiffness of the soil tends to increase. The damping and stiffness of soil depend on the soil relative density.

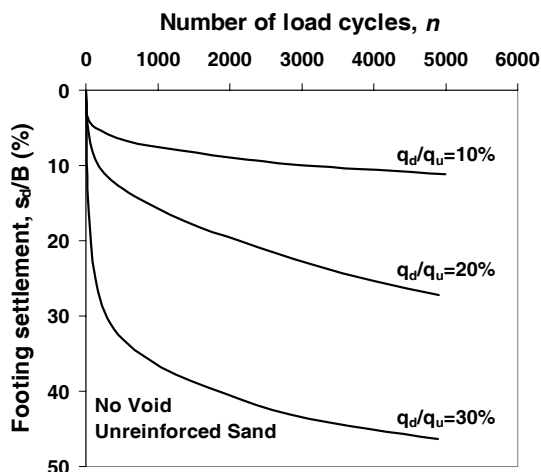


Fig. 8. Variation of footing settlement ( $s_d/B$ ) with number of loading cyclic for unreinforced sand and no void condition

### 7.2.2. The influence of the number of reinforcement layers

Fig. 9 presents the variation of the footing settlement with number of load cycles for void embedded at 2.5D (the results for  $H/D=2$  and 3 not reported here), different numbers of reinforcement layers, and various dynamic pressure amplitudes,  $q_d/q_u$ . As seen, in the case of unreinforced bed, the presence of the void increases the footing settlement, considerably. This figure shows that the reinforcements are effective on the footing settlement reduction and the

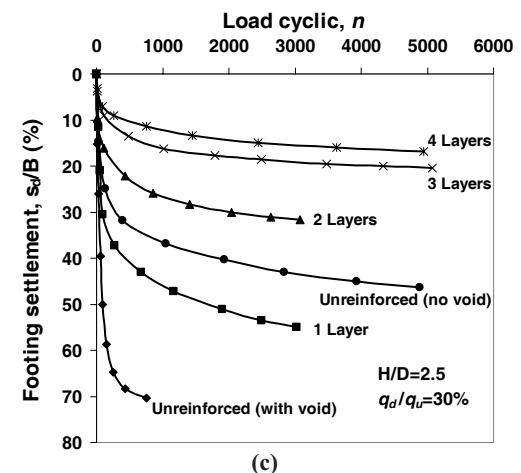
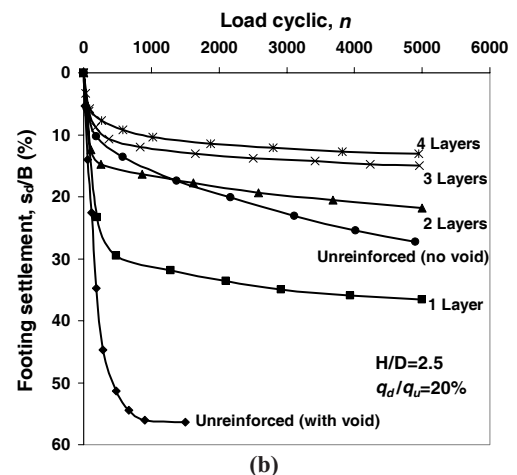
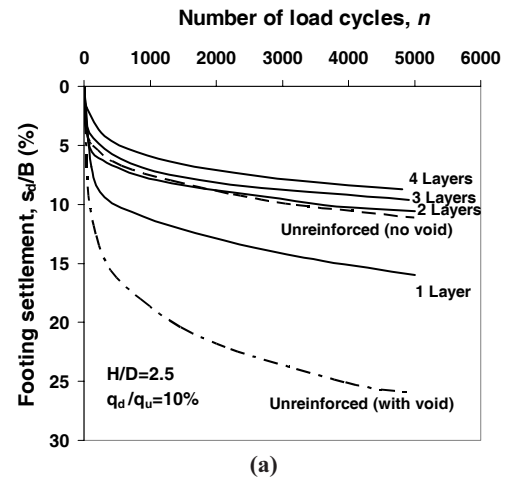


Fig. 9. Variation of settlement with number of loading cycles for footing on unreinforced and reinforced sand,  $H/D=2.5$ , (a)  $q_d/q_u=10\%$ , (b)  $q_d/q_u=20\%$ , and (c)  $q_d/q_u=30\%$



undesirable effect of the void presence is reduced with increasing the number of reinforcement. At low applied pressures ( $q_d/q_u=10\%$ ), the footing settlement decreases rapidly and by using two geogrid layers, undesirable effect of void vanishes. For medium applied pressures ( $q_d/q_u=20\%$ ), the optimum number of geogrid layers should be increased to 3. Since in these tests, only 4 geogrid layers were used, it is impossible to find the optimum number of layers for higher applied pressure amplitudes ( $q_d/q_u=30\%$ ). This is because the footing settlement tends to decrease even if 4 layers are used.

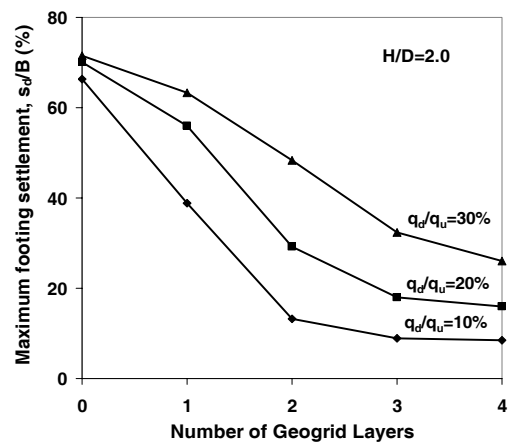
In order to clear the effect of the number of reinforcement layers on the settlement of footing on sand with void, the variation of footing settlement with number of geogrid layers ( $N$ ) for various void embedment depths,  $H/D$ , is shown in Fig. 10. As seen, with increasing the number of geogrid layers, the footing settlement decreases differently for various  $H/D$ . For  $H/D=2.0$  and  $N=3$ , the change in settlement ratio with increase the number of layers,  $N$  is insignificant and this number may be optimum denoted by  $N_{opt}$ . These values for  $H/D=2.5$  and  $3.0$  are about 2 and 1 layers, respectively. The value of  $N_{opt}$  is almost independent of the applied footing pressure, although the pressure increase causes an increase in the settlement. In fact, geogrid layers act as a bridge between the void and footing and distribute the pressure in a wider zone.

The distance between the footing bottom and the lowest geogrid layer,  $d$ , is given by:

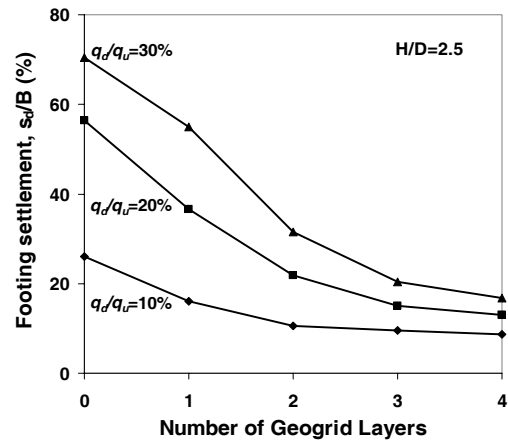
$$d = u + (N-1)h \quad (1)$$

In the present study, the values of  $(d/B)_{cr}$  were found to vary in the range of 0.7 and 1.4 for 2 and 4 layers of geogrid, respectively. However, from several studies, this ratio is about 1.33 (Das, 1998). This ratio depends on  $H/D$  and by increasing  $H/D$ , it decreases.

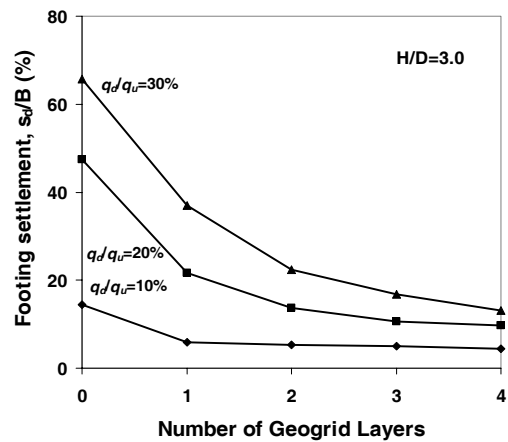
Fig. 11 shows the void failure and the void crest deformation for the tests with one, two and four layers of reinforcement for  $q_d/q_u=20\%$  and  $H/D=2.0$ . As illustrated, the number of reinforcement layers has a remarkable influence on the void failure type. It shows clearly that with increasing the reinforcement layers beneath the footing over the void, the stability of the void increases. Also with increasing the layers to 4, the void remains stable and undesirable effect of the void presence on the footing settlement completely vanishes (Fig. 9). Moreover, it indicates that there exists a direct relationship between stability of the void with the footing settlement.



(a)



(b)



(c)

Fig. 10. Variation of settlement with number of geogrid layers, (a)  $H/D=2.0$ , (b)  $H/D=2.5$ , (c)  $H/D=3.0$

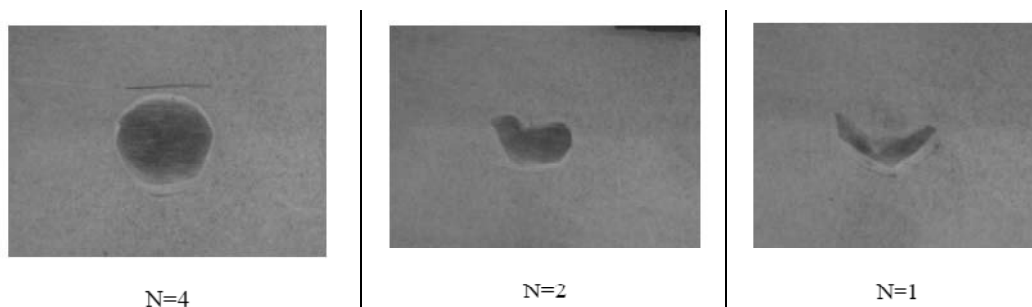


Fig. 11. Deformed void for various geogrid layers,  $q_d/q_u=20\%$  under cyclic loading, and  $H/D=2.0$

### 7.2.3. The influence of the amplitude of repeated loads

The variation of footing settlement with number of load cycles for void embedded at 3 times of void diameter,  $H/D=3.0$ , different reinforcement layers and various dynamic pressure amplitudes,  $q_d/q_u$  is shown in Fig. 12. As seen, the rate of footing settlement decreases as the number of cycles increase, and finally tends to become stable after a certain cycles, irrespective of the number of layers of reinforcement. On the other hand, the magnitude of footing settlement increases with number of cycles ( $n$ ) and reaches a sensibly constant maximum value at the number of load cycles here defined as  $n=n_{cr}$ . As expected, the increase in the magnitude of the repeated loads directly causes the footing settlement to increase, irrespective of the reinforcement mass beneath the footing. For example, the footing settlements for the foundation bed over the void with  $N=2$ , at the end of loading are 5%, 14%, and 22% of the footing width for magnitudes of repeated load that are 10%, 20%, and 30% of the initial static load, respectively (as per Fig. 12b).

Fig. 13 shows the variation of footing settlement with amplitude of repeated load for various void embedment depths and in the case of unreinforced and reinforced sand. As illustrated, the magnitude of footing settlement increases with increasing the amplitude of repeated load

considerably, irrespective of the number of reinforcement layers and void embedment depth. For  $H/D=2.0$ , when only two (or three) layers of geogrid are used with the presence of void, the footing settlement behavior is the same as the footing on unreinforced sand with no void. To reduce more settlement for  $H/D=2.0$  case, three geogrid layers should be used, especially if the factor of safety needs to increase the pressures ranging from medium and high pressures. For practical purposes,  $(d/B)_{cr}$  is equal to 1.05 for  $H/D=2.0$ . The number of geogrid layers for other ratios of  $H/D=2.5$  and 3 needs to decrease to 2 and 1 layers, respectively. The use of 2 layers of geogrid is to  $(d/B)_{cr}=0.7$  and 1 layer is equivalent to  $(d/B)_{cr}=0.35$ . In practice, if the footing settlement is to be acceptable, adequate reinforcement layers may be used to eliminate undesirable effect of the void presence. It is noted that in this study, the soil relative density was about 73%. It was found that the void became unstable if the soil density becomes less than this value.

### 7.2.4. The influence of the embedment depth of void

Fig. 14 shows the variation of footing settlement,  $s_d/B$ , in reinforced and unreinforced sand with void embedment depth for different values of reinforcement layers and for 10%, 20%, and 30% of amplitude of repeated loads,  $q_d/q_u$ . It can be seen

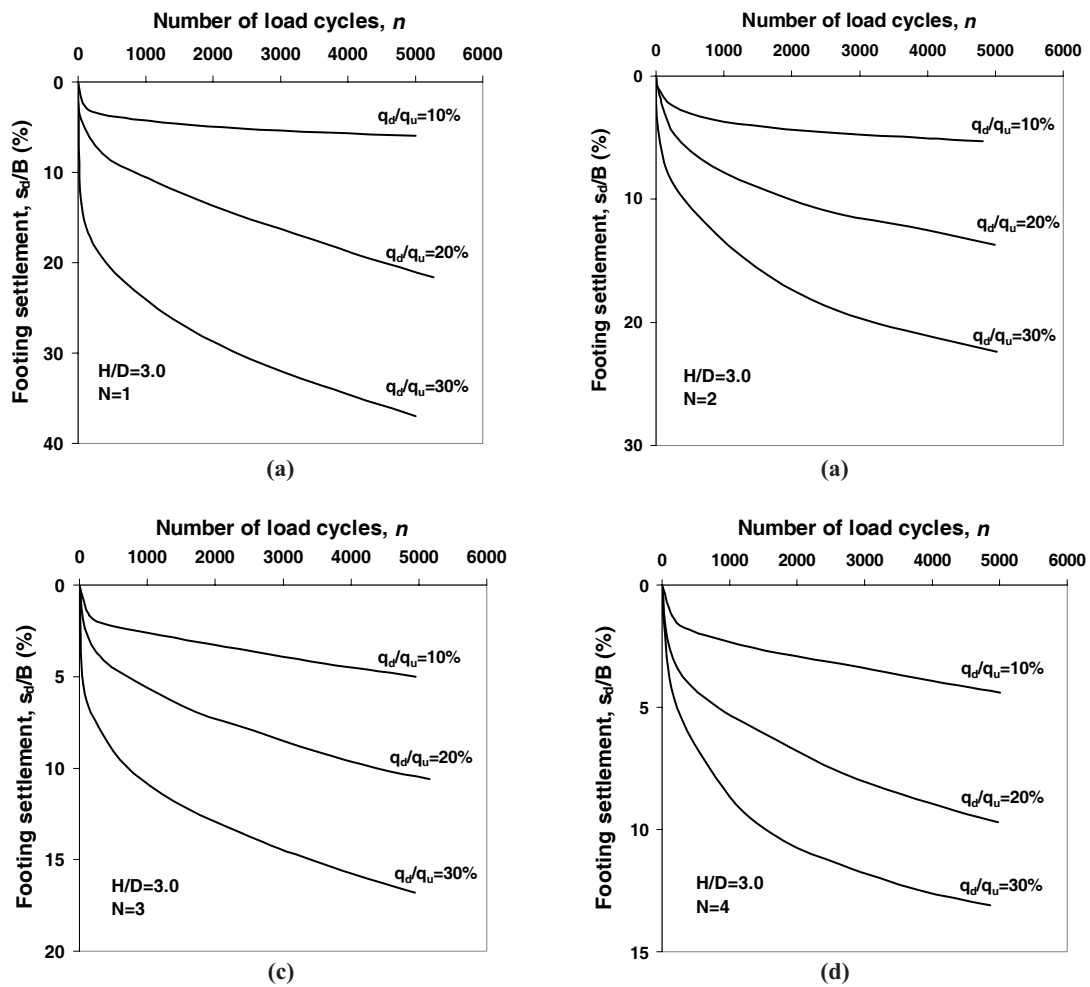


Fig. 12. Variation of settlement with number of loading cycles for  $H/D=3.0$ , various dynamic pressure amplitudes,  $q_d/q_u$ , (a) 1 layer, (b) 2 layers, (c) 3 layers, and (d) 4 layers

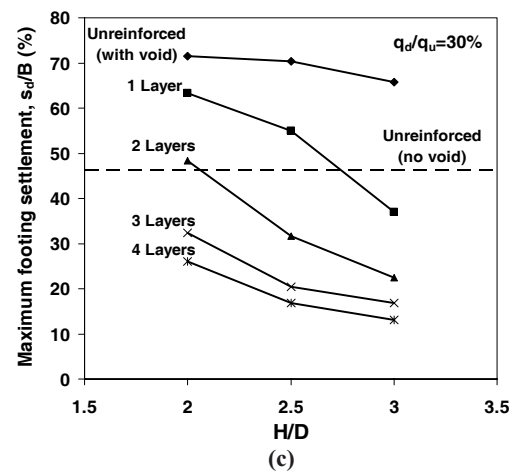
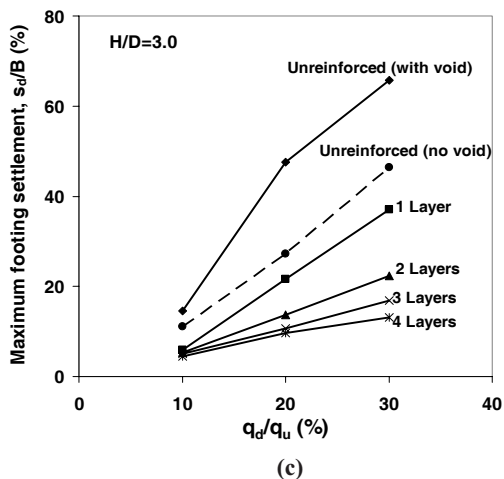
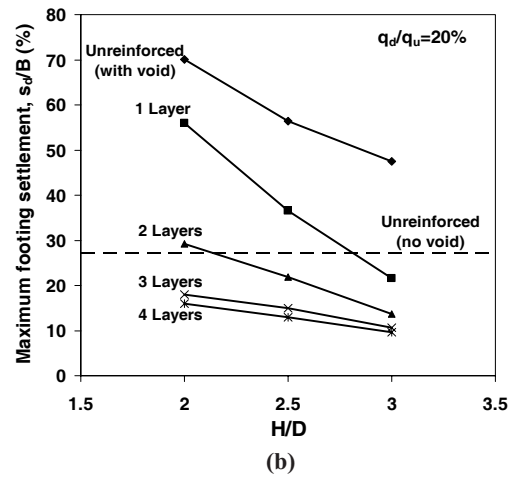
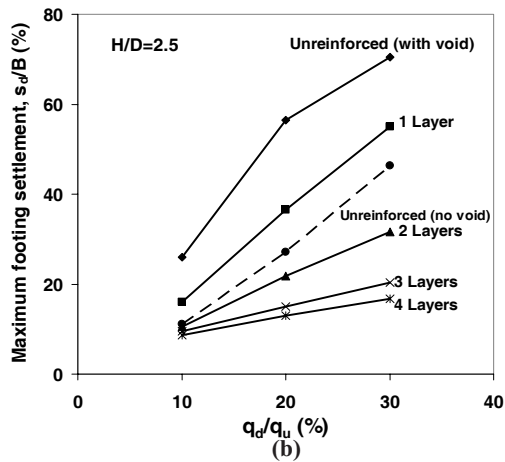
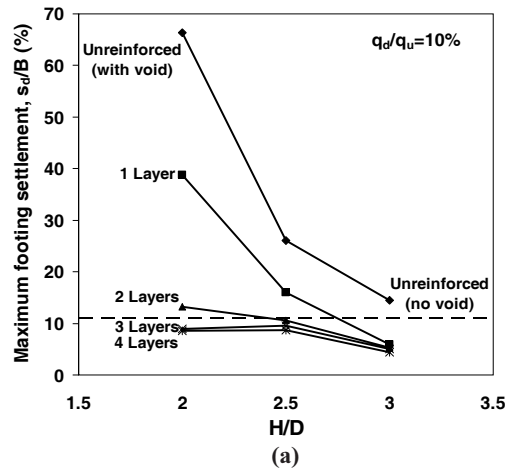
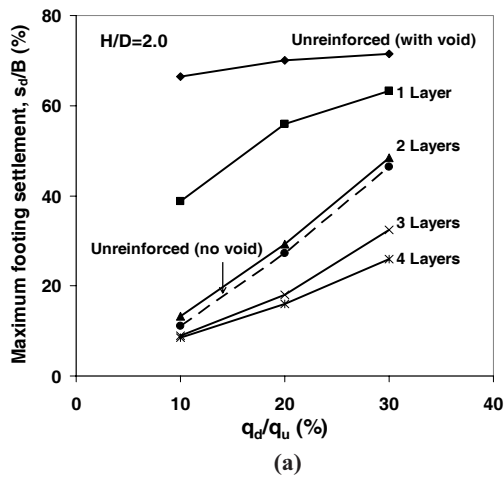


Fig. 13. Variation of settlement with ratio of loading cyclic for footing on unreinforced and reinforced sand, (a)  $H/D=2.0$ , (b)  $H/D=2.5$ , and (c)  $H/D=3.0$

Fig. 14. Variation of settlement with embedded depth of void for unreinforced and reinforced sand, (a)  $q_d/q_u=10\%$ , (b)  $q_d/q_u=20\%$ , and (c)  $q_d/q_u=30\%$

that with increasing the embedment depth of the void, the failure pattern changes and the footing settlement decreases, irrespective of the number of reinforcement layers and amplitude of repeated load. The rate of reduction in the footing settlement mostly decreases with increasing the embedment of the void, especially, at 10% of the amplitude of repeated load. Overall, for the unreinforced case and lower reinforcement layers, especially for low embedment of the void, the footing soil and the void rapidly failed and the footing

sand bed experienced significant deformation directing towards the void.

It is also clear that the increase in the mass of reinforcement could be easily vanished the undesirable effect of void to compare the footing settlement to that of an equivalent amplitude of repeated load, reference unreinforced and no void case. For instance, for  $q_d/q_u=10\%$ , when only three geogrid layers are used with the presence of void, the footing settlement is the less than the footing on

unreinforced sand with no void, irrespective of void embedment depth. In general, it may be said that to reduce the adverse effect of the void presence on the footing settlement and its bearing capacity, the void embedment depth and the number of reinforcement layers may be increased, as the void crest only deforms and no failure occurs.

7.2.5. Comparison the settlement of footing under static and repeated loads

In order to compare the footing settlement under static and repeated loads, the differential static footing settlement,  $\Delta s_s$  (difference between settlement at  $q_s+q_d$  and settlement at  $q_s$  during the static test) and repeated footing settlement,  $s_d$  are used. The definition of both parameters illustrated in Fig. 15.

Figs. 16-17 show the variation of normalized cyclic footing settlement,  $s_d/B$  and normalized differential static footing settlement,  $\Delta s_s/B$ , respectively for two and four layers of reinforcement at different void embedment depths of 2, 2.5, and 3. The values of  $s_d/B$  evaluated under repeated loading,  $q_d$  compared to  $\Delta s_s/B$  under a similar intensity of static loading,  $\Delta q_s=q_d$ .

It should be noted that at low amplitude of repeated load of about 10% of the footing ultimate bearing pressure for

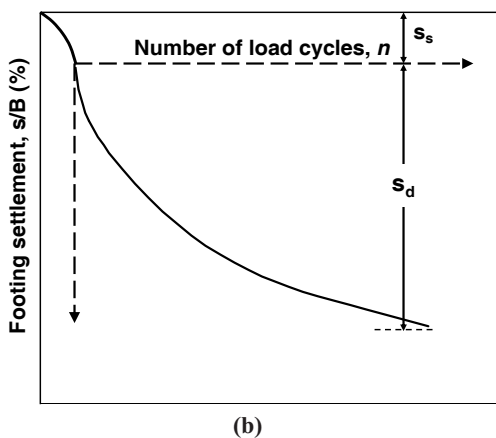
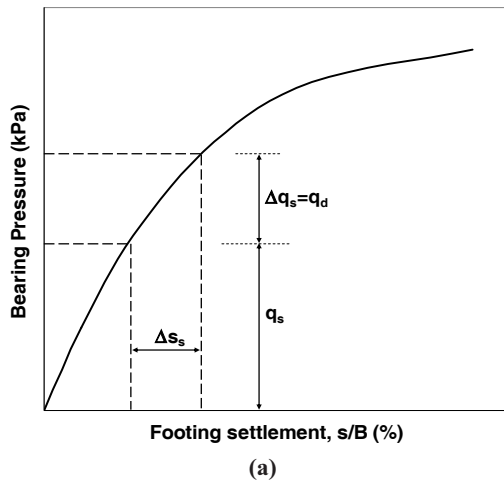


Fig. 15. Definition of (a) differential static footing  $\Delta$  settlement,  $\Delta s_s$  and (b) repeated footing settlement,  $s_d$

unreinforced sand with no void ( $q_u$ ), the total amplitude of the applied loading,  $q_s+q_d$ , is equal to  $0.43q_u$  in the same conditions. At medium and high repeated loads of 20% and 30%, the total applied loads were about  $0.53q_u$  and  $0.63q_u$ , respectively.

As observed, for various applied loads, the normalized cyclic footing settlement,  $s_d/B$  varies about 3-5 times of normalized cyclic footing settlement;  $\Delta s_s/B$  under a similar static loading. That's why the repeated loading is applied repeatedly so that

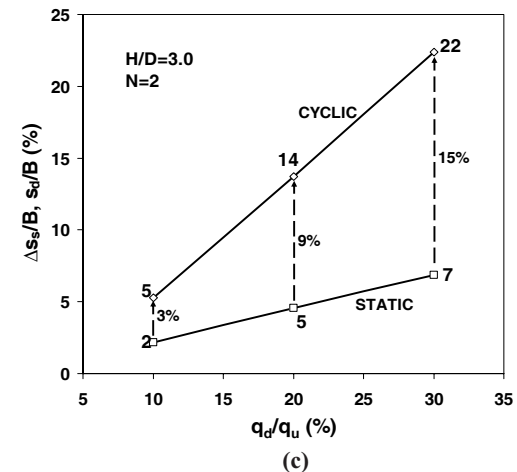
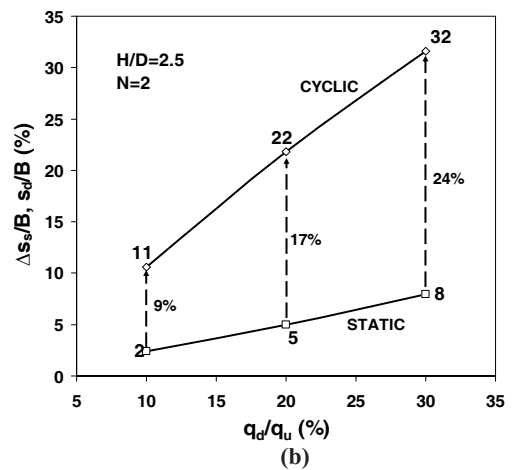
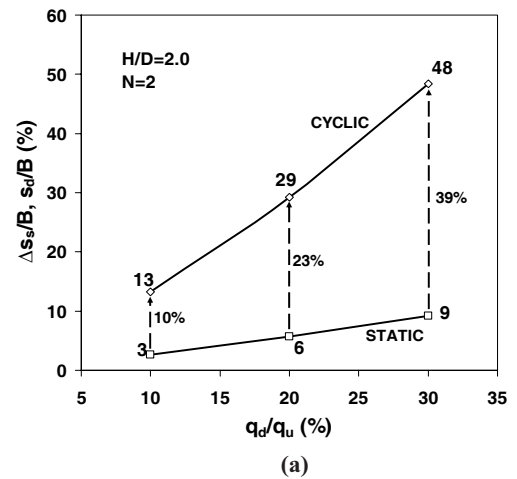


Fig. 16. Variation of cyclic footing settlement and static footing versus the same amount of cyclic and static load of footing on 2 layers reinforced sand, (a)  $H/D=2.0$ , (b)  $H/D=2.5$ , and (c)  $H/D=3.0$

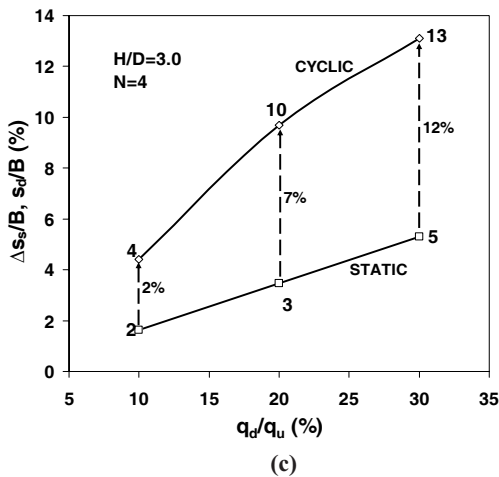
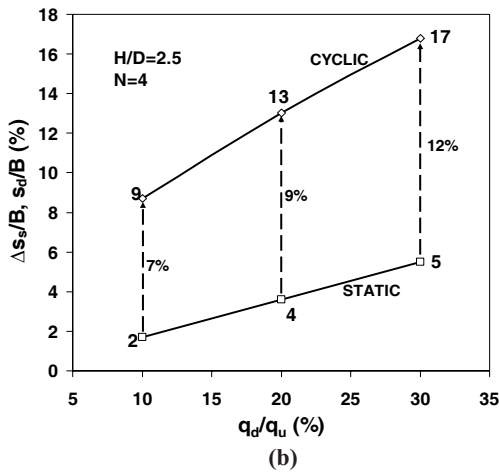
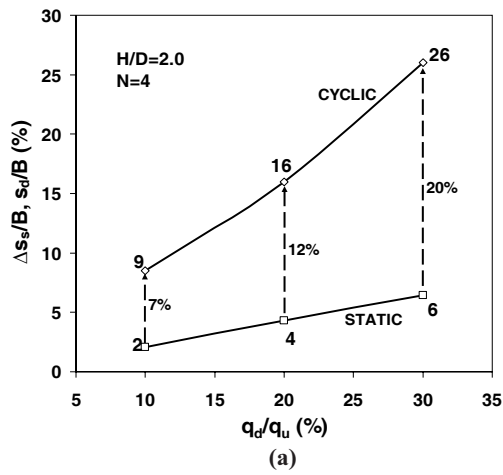


Fig. 17. Variation of cyclic footing settlement and static footing versus the same amount of cyclic and static load of footing on 4 layers reinforced sand, (a)  $H/D=2.0$ , (b)  $H/D=2.5$ , (c)  $H/D=3.0$

the accumulated plastic deformation due to many repetitions ends up much greater than that occurs under simple monotonic static loading.

### 8. Limitation and applicability

The current experiments reveal the beneficial application of sand-reinforced with geogrids, carrying cyclic loading of

footings. Qualitatively, this study has provided informative insight into the basic mechanism that occurs for footings on reinforced and unreinforced sand with or without void under cyclic loading. Although this research work encourages the beneficial application of the soil reinforcement above the void under dynamic loading, it should be noted that the results are limited to the selected materials, experimental set up geometry, and testing procedure. To generalize findings in this paper, further tests with other geometries and materials are also required. In addition, sophisticated analyses such as numerical methods are also useful to discover the role of contributing parameters.

### 9. Summary and conclusions

In this research, a series of laboratory cyclic load tests was performed on model footings on unreinforced and geogrid reinforced sand with/without void. The benefits were assessed in terms of reduced settlement of a strip footing subjected to a combination of static and cyclic loads. The following remarks may be cited as outcomes:

1. The rate of footing settlement decreases significantly with increasing the number of load cycles. As a result, a resilient response condition is achieved after about 3000-5000 cycles dependent on the void embedment depth, number of reinforcement layers and applied cyclic load magnitude.

2. For all tests, the largest portion of the footing settlement occurs within the first 500 cycles.

3. The magnitude of the maximum footing settlement and the number of cycles required to develop the stable response condition of the footing are a function of the initial applied static load ( $q_s$ ), the amplitude of the repeated load ( $q_d$ ), the embedment depth of void and the mass of reinforcement layers below the footing base.

4. For a given amplitude of cyclic load, with increasing the number of reinforcement layers and with increasing the embedment depth of void to a certain value, the footing settlement decreases.

5. With increasing the amplitude of cyclic load, the footing settlement increases, considerably.

6. The maximum footing settlement at the same magnitude of load,  $s/B$ , under cyclic loading becomes almost 3-5 times greater than that due to static loading.

7. Overall, with increasing the layers of reinforcement, embedment depth of void (or combination of these two factors), the undesirable effect of void could be vanished. On the other hand, the footing settlement becomes smaller than the footing settlement on unreinforced sand and no void condition as the void crest may only deform and no failure occurs.

8. Both the number of reinforcement layers and the void embedment depth ( $N$  and  $H/D$ ) have a large influence on the footing behavior under static and repeated load, as increasing of these two parameters can reduce the footing settlement. Hence to control the magnitude of footing settlement under static load and different intensity of repeated load, it is necessary to consider the cost optimization and its applicability.

## Nomenclature

|              |  |
|--------------|--|
| $B$          | width of footing   |
| $b$          | reinforcement width  |
| $u$          | depth of the first layer of reinforcement  |
| $h$          | vertical spacing between layers of reinforcement   |
| $N$          | number of reinforcement layers   |
| $N_{opt}$    | optimum number of reinforcement layers   |
| $n$          | number of load cycles  |
| $n_{cr}$     | maximum number of load cycles  |
| $H$          | void embedment depth   |
| $D$          | void diameter  |
| $d$          | thickness of the reinforced zone   |
| $D_r$        | relative density of soil   |
| $q_u$        | ultimate bearing pressure of footing on the unreinforced sand                              |
| $q_s$        | intensity of pre-specified static load   |
| $q_d$        | amplitude of repeated load   |
|              | intensity of static load equals the amplitude of repeated load ( $\Delta q_s = q_d$ )      |
| $\Delta q_s$ | load   |
| $\Delta s_s$ | deference between settlement at $q_s + q_d$ and settlement at $q_s$ during the static test |
| $s_d$        | maximum value of settlement of footing under repeated loads                                |

## References

- [1] Baus, R. L.; Wang, M. C., 1983. Bearing capacity of strip footings above void. *Journal of Geotechnical Engineering*, 109 (1), 1-14.
- [2] Badie, A.; Wang, M. C., 1984. Stability of spread footings above void in clay. *Journal of Geotechnical Engineering*, 110 (11), 1591-1605.
- [3] Wang, M. C., Hsieh, C. W., 1987. Collapse load of strip footing above circular void. *Journal of Geotechnical Engineering*, 113 (5), 511-515.
- [4] Wang, M. C., Yoo C. S., Hsieh C. W., 1991. Effect of Void on Footing Behavior under Eccentric and Inclined Loads. *Foundation Eng. Journal, ASCE*, 1226-1239.
- [5] Shin, E.C., Das, B.M., 2000. Experimental study of bearing capacity of a strip foundation on geogrid-reinforced sand. *Geosynthetics International*, 7 (1), 59-71.
- [6] Dash, S.K., Rajagopal, K., Krishnaswamy, N.R., 2004. Performance of different geosynthetic reinforcement materials in sand foundations. *Geosynthetics International*, 11 (1), 35-42.
- [7] Yoon, Y.W., Cheon, S.H., Kang, D.S., 2004. Bearing capacity and settlement of tire reinforced sands. *Geotextiles and Geomembranes*, 22 (5), 439-453.
- [8] Deb, K., Chandra, S., Basudhar, P.K., 2005. Settlement response of a multi layer geosynthetic-reinforced granular II- soft soil system. *Geosynthetics International*, 12 (6), 288-298.
- [9] Ghosh, A., Ghosh, A., Bera, A.K., 2005. Bearing capacity of square footing on pond ash reinforced with jute-geotextile. *Geotextiles and Geomembranes*, 23 (2), 144-173.
- [10] Patra, C.R., Das, B.M., Atalar, C., 2005. Bearing capacity of embedded strip foundation on geogrid reinforced sand. *Geotextiles and Geomembranes*, 23 (5), 454-462.
- [11] Patra, C.R., Das, B.M., Bohi, M., Shin, E.C., 2006. Eccentrically loaded strip foundation on geogrid-reinforced sand. *Geotextiles and Geomembranes*, 24 (4), 254-259.
- [12] Hufenus, R., Rueegger, R., Banjac, R., Mayor, P., Springman, S.M., Bronnimann, R., 2006. Full-scale field tests on geosynthetic reinforced unpaved on soft subgrade. *Geotextiles and Geomembranes*, 24 (1), 21-37.
- [13] El Sawwaf, M.A., 2007. Behaviour of strip footing on geogrid-reinforced sand over a soft clay slope. *Geotextiles and Geomembranes*, 25 (1), 50-60.
- [14] Alamshahi, S., Hataf, N., 2009. Bearing capacity of strip footings on sand slopes reinforced with geogrid and grid-anchor. *Geotextiles and Geomembranes*, 27 (3), 217-226.
- [15] Bathurst, R.J., Nernheim, A., Walters, D.L., Allen, T.M., Burgess, P., Saunders, D.D., 2009. Influence of reinforcement stiffness and compaction on the performance of four geosynthetic-reinforced soil walls. *Geosynthetics International*, 16 (1), 43-49.
- [16] Sharma, R., Chen, Q., AbuFarsakh, M., Yoon, S., 2009. Analytical modeling of geogrid reinforced soil foundation. *Geotextiles and Geomembranes*, 27 (1), 63-72.
- [17] Ghazavi, M., Alimardani Lavasan, A., 2008. Interference effect of shallow foundations constructed on sand reinforced with geosynthetics. *Geotextiles and Geomembranes*, 26(5), 404-415.
- [18] Nayeri, A., Fakharian, K., 2009. Study on Pullout Behavior of Uniaxial HDPE geogrids Under Monotonic and Cyclic Loads. *International Journal of Civil Engineering*. Vol. 7, No. 4, pp. 211-223.
- [19] Abdi, M.R., Sadrnejad, S.A., and Arjomand, M.A., 2009. Clay Reinforcement Using geogrid Embedded In Thin Layers of Sand. *International Journal of Civil Engineering*. Vol. 7, No. 4, pp. 224-235.
- [20] Moghaddas Tafreshi, S.N., Dawson, A.R., 2010a. Comparison of bearing capacity of a strip footing on sand with geocell and with planar forms of geotextile reinforcement. *Geotextiles and Geomembranes*, 28 (1), 72-84.
- [21] Moghaddas Tafreshi, S.N., Dawson, A.R., 2010b. Behaviour of footings on reinforced sand subjected to repeated loading - Comparing use of 3D and planar geotextile. *Geotextile and Geomembranes*, 28 (5), 434-447.
- [22] Cunny, R.W., Sloan, R.C., 1961. Dynamic loading machine and results of preliminary small-scale footing test. *Symposium on Soil Dynamics*. ASTM Special Technical Publication. No. 305, 65-77.
- [23] Raymond, G.P., Komos, F.E., 1978. Repeated load testing on a model plane strain footing. *Canadian Geotechnical Journal*, 15 (2), 190-201.
- [24] Das, B.M., Shin, E.C., 1996. Laboratory model tests for cyclic load-induced settlement of a strip foundation on clayey soil. *Geotechnical and Geological Engineering*, 14 (3), 213-225.
- [25] Das, B.M., Shin, E.C., 1994. Strip foundation on geogrid-reinforced clay: behavior under cyclic loading. *Geotextiles and Geomembranes*, 13 (10), 657-667.
- [26] Raymond, G.P., 2002. Reinforced ballast behaviour subjected to repeated load. *Geotextiles and Geomembranes*, 20 (1), 39-61.
- [27] Shin, E.C., Kim, D.H., Das, B.M., 2002. Geogrid-reinforced railroad bed settlement due to cyclic load. *Geotechnical and Geological Engineering*, 20 (3), 261-271.
- [28] Moghaddas Tafreshi, S.N., Khalaj, O., 2008. Laboratory tests of small-diameter HDPE pipes buried in reinforced sand under repeated load. *Geotextiles and Geomembranes*, 26 (2), 145-163.
- [29] Moghaddas Tafreshi, S.N., Tavakoli Mehrjardi, G., Moghaddas Tafreshi, S.M., 2007. Analysis of Buried Plastic Pipes in Reinforced Sand under Repeated-Load Using Neural Network and Regression Model. *International Journal of Civil Engineering*. Vol. 5, No. 2, pp. 118-133.
- [30] Das, B.M., Maji, A., 1994. Transient loading related settlement of a square foundation on geogrid-reinforced sand. *Geotechnical and Geological Engineering*, 12 (4), 241-251.

- [31] Das, B.M., 1998. Dynamic loading on foundation on reinforced sand. geosynthetics in foundation reinforcement and erosion control systems. American Society of Civil Engineers 76, 19-33.
- [32] Das, B.M., Khing, K.H., 1994. Foundation on layered soil with geogrid reinforcement effect of a void. Geotextiles and Geomembranes 13 (8), 545-553.
- [33] Wang, M.C., Feng, Y.X., Jao, M., 1996. Stability of geosynthetic-reinforced soil above a cavity. Geotextiles and Geomembranes, 14, No. 2, 95-109.
- [34] Briancon, L., Villard, P., 2008. Design of geosynthetic-reinforced platforms spanning localized sinkholes. Geotextiles and Geomembranes, 26, No. 5, 416-428.
- [35] Sireesh, S., Sitharam, T.G., Dash, S.K., 2009. Bearing capacity of circular footing on geocell-sand mattress overlying clay bed with void. Geotextiles and Geomembranes, 27 (2), 89-98.
- [36] Kolbuszewski, J. 1948. General investigation of the fundamental factors controlling loose packing of sands. In: Proc. of the 2nd Int. Conf. on Soil Mech. and found Eng., Rotterdam, vol. VII, pp. 47-49.
- [37] Hoeg, K., 1965. Pressure distribution on underground structural cylinders. Ph.D Thesis, Massachusetts, USA.



این مقاله، از سری مقالات ترجمه شده رایگان سایت ترجمه فا میباشد که با فرمت PDF در اختیار شما عزیزان قرار گرفته است. در صورت تمایل میتوانید با کلیک بر روی دکمه های زیر از سایر مقالات نیز استفاده نمایید:

لیست مقالات ترجمه شده ✓

لیست مقالات ترجمه شده رایگان ✓

لیست جدیدترین مقالات انگلیسی ISI ✓

سایت ترجمه فا ؛ مرجع جدیدترین مقالات ترجمه شده از نشریات معتبر خارجی